

## Detection of Pionium with DIRAC

A. Lanaro

*CERN, Geneva, Switzerland, and INFN-Laboratori Nazionali di Frascati, Frascati, Italy*

on behalf of

“The DIRAC Collaboration”

B. Adeva<sup>o</sup>, L. Afanasev<sup>l</sup>, M. Benayoun<sup>d</sup>, V. Brekhovskikh<sup>n</sup>,  
 G. Caragheorghopol<sup>m</sup>, T. Cechak<sup>b</sup>, M. Chiba<sup>j</sup>, S. Constantinescu<sup>m</sup>, A. Doudarev<sup>l</sup>,  
 D. Dreossi<sup>f</sup>, D. Drijard<sup>a</sup>, M. Ferro-Luzzi<sup>a</sup>, T. Gallas Torreira<sup>a,o</sup>, J. Gerndt<sup>b</sup>,  
 R. Giacomich<sup>f</sup>, P. Gianotti<sup>e</sup>, F. Gomez<sup>o</sup>, A. Gorin<sup>n</sup>, O. Gortchakov<sup>l</sup>, C. Guaraldo<sup>e</sup>,  
 M. Hansroul<sup>a</sup>, R. Hosek<sup>b</sup>, M. Iliescu<sup>e,m</sup>, N. Kalinina<sup>l</sup>, V. Karpoukhine<sup>l</sup>, J. Kluson<sup>b</sup>,  
 M. Kobayashi<sup>g</sup>, P. Kokkas<sup>p</sup>, V. Komarov<sup>l</sup>, A. Koulikov<sup>l</sup>, A. Kouptsov<sup>l</sup>, V. Krouglov<sup>l</sup>,  
 L. Krouglova<sup>l</sup>, K.-I. Kuroda<sup>k</sup>, A. Lanaro<sup>a,e</sup>, V. Lapshin<sup>n</sup>, R. Lednicky<sup>c</sup>, P. Leruste<sup>d</sup>,  
 P. Levisandri<sup>e</sup>, A. Lopez Aguera<sup>o</sup>, V. Lucherini<sup>e</sup>, T. Maki<sup>i</sup>, I. Manuilov<sup>n</sup>, L. Montanet<sup>a</sup>,  
 J.-L. Narjoux<sup>d</sup>, L. Nemenov<sup>a,l</sup>, M. Nikitin<sup>l</sup>, T. Nunez Pardo<sup>o</sup>, K. Okada<sup>h</sup>, V. Olchevskii<sup>l</sup>,  
 A. Pazos<sup>o</sup>, M. Pentic<sup>m</sup>, A. Penzo<sup>f</sup>, J.-M. Perreau<sup>a</sup>, C. Petrascu<sup>e,m</sup>, M. Plo<sup>o</sup>, T. Ponta<sup>m</sup>,  
 D. Pop<sup>m</sup>, A. Riazantsev<sup>n</sup>, J.M. Rodriguez<sup>o</sup>, A. Rodriguez Fernandez<sup>o</sup>, V. Rykaline<sup>n</sup>,  
 C. Santamarina<sup>o</sup>, J. Schacher<sup>q</sup>, A. Sidorov<sup>n</sup>, J. Smolik<sup>c</sup>, F. Takeutchi<sup>h</sup>, A. Tarasov<sup>l</sup>,  
 L. Tauscher<sup>p</sup>, S. Trousov<sup>l</sup>, P. Vazquez<sup>o</sup>, S. Vlachos<sup>p</sup>, V. Yazkov<sup>l</sup>, Y. Yoshimura<sup>g</sup>,  
 P. Zrelov<sup>l</sup>

<sup>a</sup> CERN, Geneva, Switzerland

<sup>b</sup> Czech Technical University, Prague, Czech Republic

<sup>c</sup> Prague University, Czech Republic

<sup>d</sup> LPNHE des Universites Paris VI/VII, IN2P3-CNRS, France

<sup>e</sup> INFN - Laboratori Nazionali di Frascati, Frascati, Italy

<sup>f</sup> Trieste University and INFN-Trieste, Italy

<sup>g</sup> KEK, Tsukuba, Japan

<sup>h</sup> Kyoto Sangyou University, Japan

<sup>i</sup> UOEH-Kyushu, Japan

<sup>j</sup> Tokyo Metropolitan University, Japan

<sup>k</sup> Waseda University, Japan

<sup>l</sup> JINR Dubna, Russia

<sup>m</sup> National Institute for Physics and Nuclear Engineering IFIN-HH, Bucharest, Romania

<sup>n</sup> IHEP Protvino, Russia

<sup>o</sup> Santiago de Compostela University, Spain

<sup>p</sup> Basel University, Switzerland

<sup>q</sup> Bern University, Switzerland

### Abstract

The aim of the DIRAC experiment at CERN is to provide an accurate determination of S-wave  $\pi\pi$  scattering lengths from the measurement of the lifetime of the  $\pi^+\pi^-$  atom. The measurement will be done with precision comparable to the level of accuracy of theoretical predictions, formulated in the context of Chiral Perturbation Theory. Therefore, the understanding of chiral symmetry breaking of QCD will be submitted to a stringent test.

### INTRODUCTION

The low-energy dynamics of strongly interacting hadrons is under the domain of non-perturbative QCD, or QCD in the confinement region. At present, low energy pion-pion scattering is still an unresolved problem in the context of QCD. However, the approach based on effective chiral Lagrangian has been able to provide accurate predictions on

the dynamics of light hadron interactions [1]. In particular, Chiral Perturbation Theory (CHPT) allows to predict the S-wave  $\pi\pi$  scattering lengths at the level of few percent [2]. Available experimental results, on their side, are much less accurate than theoretical predictions, both because of large experimental uncertainty and, in some cases, unresolved model dependency [3].

The DIRAC experiment aims at a model independent measurement of the difference  $\Delta$  between the isoscalar  $a_0$  and isotensor  $a_2$  S-wave  $\pi\pi$  scattering lengths with 5% precision, by measuring the lifetime of the pionium ground state with 10% precision.

## PIONIUM

Pionium ( $A_{2\pi}$ ) is a Coulomb weakly-bound system of a  $\pi^+$  and a  $\pi^-$ , whose lifetime is dominated by the charge-exchange process to two neutral pions. The Bohr radius is 387 fm, the Bohr momentum 0.5 MeV/c, and the binding energy 1.86 keV. The decay probability is proportional to the atom wave function squared at zero pion separation and to the square of  $\Delta = a_0 - a_2$ . Using the values of scattering lengths predicted by CHPT, the lifetime of the  $\pi^+\pi^-$  atom in the ground state is predicted to be  $3.25 \times 10^{-15}$  s [2].

### Production of $A_{2\pi}$

In DIRAC,  $\pi^+\pi^-$  atoms are formed by the interaction of 24 GeV/c protons with nuclei in thin targets [4]. If two final state pions have a small relative momentum in their system ( $q \sim 1\text{MeV}/c$ ), and are much closer than the Bohr radius, then the  $A_{2\pi}$  production probability, due to the high overlap, is large. Such pions originate from short-lived sources (like  $\rho$  and  $\omega$ ), but not from long-lived ( $\eta$ ,  $K_s^0$ ), because in the latter case the two-pion separation is larger than the Bohr radius. The production probability for  $A_{2\pi}$  can then be calculated using the double inclusive production cross section for  $\pi^+\pi^-$  pairs from short-lived sources, excluding Coulomb interaction in the final state [5]. Evidence for  $A_{2\pi}$  production was reported in a previous experiment [6].

### Fate of $A_{2\pi}$

Pionium travelling in matter can dissociate or break up into a pair of oppositely charged pions with small relative momentum ( $q < 3$  MeV/c) and hence with very small angular divergence ( $\theta < 0.3$  mrad). This process competes with the charge-exchange reaction or decay, if the target material is dense so that the atomic interaction length is similar to the typical decay length of a few GeV/c dimeson atom (a few tens of microns). In a  $100\mu\text{m}$  Ni foil, for example, the  $A_{2\pi}$  breakup probability ( $\sim 47\%$ ) becomes larger than the annihilation probability ( $\sim 38\%$ ). This breakup probability depends on the target nucleus charge  $Z$ , the target thickness, the  $A_{2\pi}$  momentum, and on the  $A_{2\pi}$  lifetime [5,7].

### Measurement of the $A_{2\pi}$ lifetime

For a target material of a given thickness, the breakup probability for pionium can be experimentally determined from the measured ratio of the number of dissociated atoms ( $n_A$ ) to the calculated number of produced  $A_{2\pi}$  ( $N_A$ ). Thus, by comparison with the theoretical value, known at the 1% level, the  $A_{2\pi}$  lifetime can be determined.

The number  $n_A$  of detected “atomic pairs” is obtained from the experimental distribution of relative momenta  $q$  for pairs of oppositely charged pions. It is however necessary to subtract a background contribution, arising mainly from Coulomb-correlated pions pairs in the  $q$  region, where the  $A_{2\pi}$  signal is prominent ( $q < 2$  MeV/c). The low- $q$  background contribution is obtained with an extrapolation procedure using the shape of the accidental pair  $q$ -distribution recorded in the region  $q > 3$  MeV/c, taking into account e.m. and strong  $\pi^+\pi^-$  final state interactions [7].

From the measured ratio  $n_A/N_A$  a value for the  $A_{2\pi}$  ground state lifetime can be extracted and, hence, a value for  $\Delta = |a_0 - a_2|$ .

## THE EXPERIMENTAL APPARATUS

The DIRAC experimental apparatus (Fig. 1) [4], devoted to the detection of charged pion pairs, was installed and commissioned in 1998 at the ZT8 beam area of the PS East Hall at CERN. After a calibration run at the end of 1998, DIRAC has been collecting data since the summer of 1999.

The primary PS proton beam of 24 GeV/c nominal momentum struck the DIRAC target. The non-interacting beam travels below the secondary particle channel (tilted upwards at  $5.7^\circ$  with respect to the proton beam), until it is absorbed by a catcher downstream of the setup. Downstream the experimental target, secondary particles travel across the following detectors: three planes of Micro-Strip Gas Chambers (MSGC) and two orthogonal stacks of scintillating fibers (Scintillating Fiber Detector SFD) to provide tracking information upstream of the spectrometer magnet; two planes of vertical scintillator slabs (Ionization Hodoscope IH) to detect the particle energy loss. Downstream the IH, the secondary beam enters a vacuum channel extending through the poles of the spectrometer magnet of 2.3 Tm bending power in the tilted horizontal plane. Downstream the analyzing magnet, the setup splits into two arms (inclined by  $5.7^\circ$  in the vertical plane, and open by  $\pm 19^\circ$  in the horizontal plane) equipped with a set of identical detectors: 14 drift chamber (DC) planes, one plane of vertical scintillating strips (Vertical Hodoscope VH) and one of horizontal strips (Horizontal Hodoscope HH) for tracking purposes downstream of the magnet; furthermore, a  $N_2$  gas-threshold Cherenkov counter (CH), a Pre-Shower Detector (PS), consisting of Pb converter plates and of vertical scintillator slabs, and a Muon counter (MU), consisting of an array of vertical scintillator elements placed behind a block of iron absorber, with the aim of performing particle identification at the trigger or offline levels.

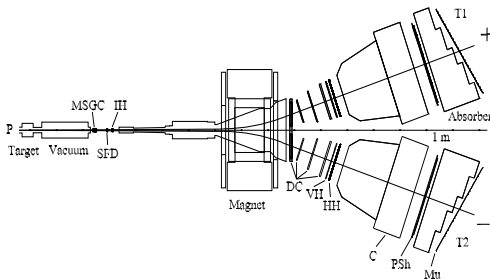


Fig. 1. The DIRAC experimental apparatus.

A multi-level trigger was designed to reduce the secondary particles rate to a level manageable by the data acquisition system, and to yield the most favorable signal-to-noise ratio, by selecting pion pairs with low relative momentum in the pair system (or small opening angle and equal energies in the lab system) and by recording a sufficiently large number of accidental pairs for the offline analysis. An incoming flux of  $\sim 10^{11}$  protons/s would produce a rate of secondaries of about  $3 \times 10^6$ /s and  $1.5 \times 10^6$ /s in the upstream and downstream detectors, respectively. At the trigger level this rate is reduced to about  $2 \times 10^3$ /s, with an average event size of about 0.75 Kbytes. With the  $95 \mu\text{m}$  thin Ni target, the expected average  $A_{2\pi}$  yield in the geometrical and momentum setup acceptance is  $\sim 0.7 \times 10^{-3}$ /s, equivalent to a total number of  $\sim 10^{13}$  protons on target to produce one dimeson atom.

## RESULTS FROM FIRST DATA TAKING

A preliminary analysis was performed on a sample of data (Ni target) collected during this summer. The sample consisted of about  $10^7$  events, corresponding to  $\sim 1/3$  of the statistics, accumulated in a 3-week run period. The data analysis was mostly dedicated

to the calibration of individual detectors and to the tuning of reconstruction algorithms. However, some general features of the apparatus response were investigated, and some results will be presented hereafter.

Figure 2 shows the time difference between hit slabs in the left and right vertical hodoscopes for events with one single track reconstructed in each detector arm. Within a trigger window of 45 ns, one observes the peak of “on-time” hits associated to correlated particles, over the background from accidental hits. The width of the correlated-pair events yields the time resolution of the hodoscope ( $\sigma \sim 420$  ps at the time of measurement, recently improved to  $\sim 250$  ps). The asymmetry on the right of the coincidence peak is due to admixture of protons in the “ $\pi^+$ ” sample, thus corresponding to events of the type  $\pi^-p$ .

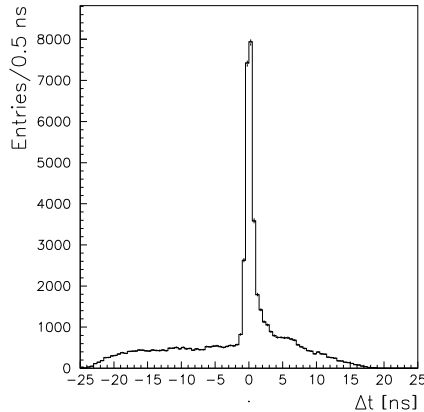


Fig. 2. Time difference between left and right VH scintillator slabs, hit by particles.

Such a contamination sample can be isolated by the time-of-flight measurement along the path from the target to the hodoscope. The discrimination between  $\pi^-\pi^+$  and  $\pi^-p$  pairs is effective for momenta of positively charged particles below 4.5 GeV/c. This is shown in Fig. 3, where the laboratory momentum of the positive particle in the pair is shown as a function of the arrival-time difference in the vertical hodoscope. The spectrometer single particle momentum acceptance is within the range 1.3 to 7.0 GeV/c.

In Fig. 4, the distribution of the longitudinal component ( $q_L$ ) of the relative momentum in the pair system is shown for two samples of events: those (Fig. 4a) occurring with time differences close to zero (real coincidence plus admixture of accidental pairs), associated to free pairs with and without final state interaction; and those (Fig. 4b) occurring at time differences far from the peak of correlated pairs (only accidental pairs).

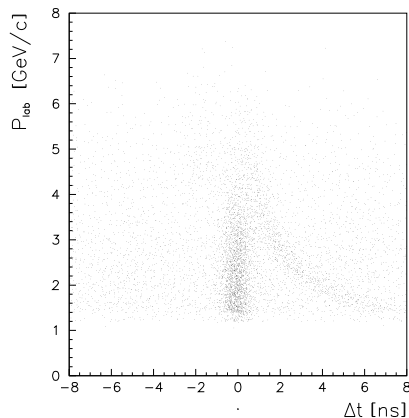


Fig. 3. Momentum of positive particle as a function of time difference between left and right hit slabs of the vertical hodoscopes.

Finally (Fig. 4c), the  $q_L$  distribution of correlated pion pairs is obtained from the difference between the distributions of Fig. 4a and 4b, taking into account the relative normalization factor. The distributions in Fig. 4 were obtained from a sample of two-track

events, preselected with momentum of the positive particle less than 4.5 GeV/c, to reject unresolved  $\pi^-p$  pairs, and with transverse component ( $q_T$ ) of the relative momentum below 4 MeV/c, to increase the fraction of low relative momentum pairs. For values of  $q_L$  corresponding to correlated pairs ( $|q_L| < 10$  MeV/c) the production cross section of Coulomb pairs is enhanced with respect to the cross section of non-Coulomb pairs: Coulomb attraction in the final state is responsible for the peak in the  $q_L$  distribution (Fig. 4a and 4c) at small  $q_L$ .

A preliminary estimate of the number of pairs associated to  $A_{2\pi}$  breakup results in a contribution of about 100 “atomic pairs” in the region  $|q_L| < 2$  MeV/c.

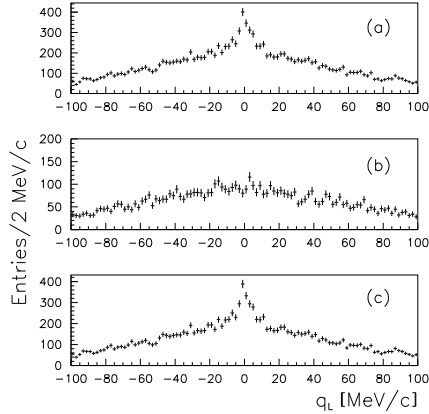


Fig. 4. Distribution of the longitudinal component of the relative momentum for: (a) time-correlated pairs; (b) accidental pairs; (c) spectrum of time-correlated minus accidental pairs.

The reconstruction of Coulomb-correlated  $\pi^+\pi^-$  pairs is sensitive to the precision of the setup alignment. Any misalignment of the tracking system in one arm relative to the other arm would generate asymmetrical errors on the reconstructed momenta. This would lead to a systematic shift and additional spread of the Coulomb enhanced peak in the  $q_L$  distribution. The mean value of the Coulomb peak is 0.1 MeV/c, well within the accepted tolerances.

When reconstructed momenta of oppositely charged particles are symmetrically overestimated or underestimated then a calibration using detected resonances is adequate. This is done by reconstructing the effective mass of  $\pi^-p$  pairs, also detected in the spectrometer. Figure 5 shows the invariant mass distribution of correlated  $\pi^-p$  pairs with proton momentum  $>3$  GeV/c.

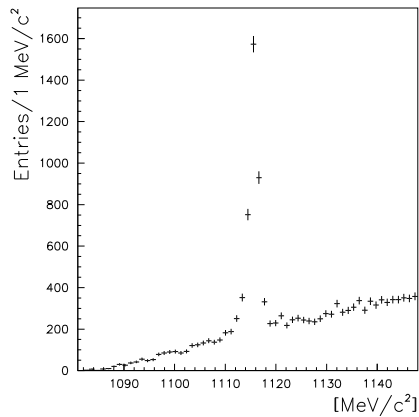


Fig. 5. Invariant mass of reconstructed  $\pi^-p$  pairs.

A clear signal at the nominal  $\Lambda$  mass is observed. Such events originate from a few GeV/c  $\Lambda$ , with the decaying proton emitted backward and the pion emitted forward in the  $\Lambda$  system, and both decay particles characterized by small transverse momenta. The experimental mean value and standard deviation of the mass peak are 1115.60 and 0.92 MeV/c<sup>2</sup>, respectively. These mass parameter values suggest an excellent calibration of

the momentum scale, with accuracy in momentum reconstruction better than 0.5% in the kinematic range of detected  $\Lambda$  decays, and the absence of errors in the telescope alignment, which otherwise would cause a displacement of the  $\Lambda$  mass peak value.

## CONCLUSION

The DIRAC experiment has begun to collect data this year. A preliminary investigation of the apparatus performances demonstrates its full capability to pursue the foreseen experimental program. Improvements to the hardware as well as software tools have already been implemented in the second run period, currently in progress. These will certainly result in better quality of the data and will contribute to the aimed measurement precision of the pionium lifetime.

## REFERENCES

1. S.Weinberg, Phys. Rev. **166**, 1569 (1968);  
S.Weinberg, Physica **96A**, 327 (1979);  
H.Leutwyler, in Proceedings of XXVI Conf. on High Energy Physics, **No.272**, Dallas, 1992 (AIP, New York, 1993) p. 185;  
J.Gasser and H.Leutwyler, Phys. Lett. **B125**, 327 (1983);  
J.Gasser and H.Leutwyler, Nucl. Phys. **B250**, 465, 517, 539 (1985);  
J.Stern, H.Sazdjian and N.H.Fuchs, Phys. Rev. **D43**, 3814 (1993);  
M.Knecht et al., Nucl. Phys. **B455**, 513 (1995).
2. J.Bijnens et al., Phys. Lett. **B374**, 210 (1996);  
D.Eiras, and J.Soto, "Effective Field Theory Approach to Pionium," CERN hep-ph/9905543 v2 (1999) and this Proceedings;  
V. Lyubovitskij, "Hadronic Atoms in QCD," this Proceedings;  
A.Rusetsky, "Isospin Breaking Effects in Bound State Observables," this Proceedings.
3. L.Rosselet et al., Phys. Rev. **D15**, 574 (1977);  
C.D.Froggat and J.L.Petersen, Nucl. Phys. **B129**, 89 (1977);  
W.Ochs, Max Planck Inst. prep. MPI-Ph/Ph 91-35, (1991);  
M.Kermani et al., Phys. Rev. **C58**, 3431 (1998).
4. B.Adeva et al., "Lifetime Measurement of  $\pi^+\pi^-$  Atoms to Test Low Energy QCD Predictions," Proposal to the SPSLC, CERN/SPSLC 95-1, SPSLC/P 284, (1994).
5. L.L.Nemenov, Yad. Fiz. **41**, 980 (1985);  
O.E.Gorchakov et al., Yad. Fiz. **59**, 2015 (1996).
6. L.G.Afanasyev et al., Phys. Lett. **B308**, 200 (1993); Phys. Lett. **B338**, 478 (1994);  
Yad. Fiz. **60**, 1049 (1996).
7. L.G.Afanasyev, JINR E2-91-578, Dubna, (1991);  
L.G.Afanasyev and A.V.Tarasov, JINR E4-93-293 Dubna, (1993).